Glycobiology vol. 16 no. 7 pp. 666–678, 2006
doi:10.1093/glycob/cwj104
Advance Access publication on March 20, 2006

Structural studies and mechanism of *Saccharomyces cerevisiae* dolichyl-phosphate-mannose synthase: insights into the initial step of synthesis of dolichyl-phosphate-linked oligosaccharide chains in membranes of endoplasmic reticulum

Ejvis Lamani[2], R. Brandon Mewbourne[2,3], Damona S. Fletcher[2,3], Sergei D. Maltsev[5], Leonid L. Danilov[5], Vladimir V. Veselovsky[5], Antonina V. Lozanova[5], Natalia Ya. Grigorieva[5], Olga A. Pinsker[5], Jun Xing[4], W. Thomas Forsee[3], Herbert C. Cheung[4], John S. Schutzbach[3], Vladimir N. Shibaev[5], and Mark J. Jedrzejas[1,2]

[2]Children's Hospital Oakland Research Institute, Oakland, CA 94609; [3]Department of Microbiology, and [4]Department of Biochemistry and Molecular Genetics, University of Alabama at Birmingham, Birmingham, AL 35294; and [5]N.D. Zelinsky Institute of Organic Chemistry, Russian Academy of Sciences, 117913 Moscow, Russia

Received on February 10, 2006; revised on March 14, 2006; accepted on March 17, 2006

Dolichyl-phosphate-mannose (Dol-P-Man) synthase catalyzes the reversible formation of a key intermediate that is involved as a mannosyl donor in at least three different pathways for the synthesis of glycoconjugates important for eukaryotic development and viability. The enzyme is found associated with membranes of the endoplasmic reticulum (ER), where it transfers mannose from the water soluble cytoplasmic donor, guanosine 5′-diphosphate (GDP)-Man, to the membrane-bound, extremely hydrophobic, and long-chain polyisoprenoid acceptor, dolichyl-phosphate (Dol-P). The enzyme from *Saccharomyces cerevisiae* has been utilized to investigate the structure and activity of the protein and interactions of the enzyme with Dol-P and synthetic Dol-P analogs containing fluorescent probes. These interactions have been explored utilizing fluorescence resonance energy transfer (FRET) to establish intramolecular distances within the protein molecule as well as intermolecular distances to determine the localization of the active site and the hydrophobic substrate on the enzyme's surface. A three-dimensional (3D) model of the enzyme was produced with bound substrates, Dol-P, GDP-Man, and divalent cations to delineate the binding sites for these substrates as well as the catalytic site. The FRET analysis was used to characterize the functional properties of the enzyme and to evaluate its modeled structure. The data allowed for proposing a molecular mechanism of catalysis as an inverting mechanism of mannosyl residue transfer.

One of the authors of this study and our friend, Professor Vladimir Nikolaevich Shibaev, unexpectedly passed away recently and we dedicate this manuscript to him and his memory.

[1]To whom correspondence should be addressed; e-mail: mjedrzejas@chori.org

Key words: dolichyl-P/GDP-mannose/membranes/molecular mechanism of action/modeling/protein glycosylation

Introduction

Dolichyl-phosphate-mannose (Dol-P-Man) synthase (EC 2.4.1.83) is a membrane enzyme located in the endoplasmic reticulum (ER), where it catalyzes the reversible transfer of mannose from the hydrophilic glycosyl-donor guanosine 5′-diphosphate (GDP)-Man to the extremely hydrophobic long-chain polyisoprenoid acceptor, dolichyl-phosphate (Dol-P) resulting in the formation of Dol-P-Man (Schutzbach, 1997; Schenk *et al.*, 2001). The ubiquitous distribution of Dol-P-Man synthase implies the key importance of this enzyme for all eukaryotic cells, where it produces a substrate that is required as a mannosyl donor in pathways for protein N-glycosylation (Schutzbach, 1997; Drickamer and Taylor, 1998; Schenk *et al.*, 2001), for protein O-glycosylation, and for the post-translational modification of proteins with glycosylphosphatidylinositol (GPI) anchors (Kinoshita *et al.*, 1997; Ferguson, 1999). The enzyme was first discovered in eukaryotes and partially purified (Tanner, 1969; Babczinski and Tanner, 1973). More recently, Dol-P-Man was demonstrated to also participate in the C-mannosylation of specific tryptophan residues (Doucey *et al.*, 1998). In humans, a partial deficiency in Dol-P-Man synthase was found to be associated with congenital disorder of glycosylation type Ie (CDG-Ie) (Imbach *et al.*, 2000; Kim *et al.*, 2000; Rush *et al.*, 2000) with severe clinical manifestations. A complete lack of Dol-P-Man synthase results in a block of GPI anchor biosynthesis, which requires Dol-P-Man (Nozaki *et al.*, 1999), and causes embryonic lethality in mice. In *Saccharomyces cerevisiae*, Dol-P-Man synthase was demonstrated to be essential for cell viability (Orlean, 1992). The gene for the enzyme codes for a protein of 267 amino acids with a single hydrophobic and potentially membrane-spanning domain near the C-terminus of the polypeptide chain (Orlean *et al.*, 1988). Its experimental three-dimensional (3D) structure still remains to be established.

The genes for Dol-P-Man synthase (*DPM1*) have been cloned from several organisms and the resultant proteins (DPM1) were found to belong to two major classes (Colussi *et al.*, 1997). Proteins of the first class, which includes enzymes from *S. cerevisiae* (Orlean *et al.*, 1988), *Ustilago maydis* (Zimmerman *et al.*, 1996), *Trypanosoma brucei* (Mazhari-Tabrizi *et al.*, 1996), and *Leishmania mexicana* (Ilgoutz *et al.*, 1999), possess a C-terminal hydrophobic sequence region and can be expressed in *Escherichia coli* as

completely functional enzymes (Orlean *et al*., 1988; Beck *et al*., 1990). The second class of enzymes is represented by the human DPM1 homolog as well as similar proteins present in *Caenorhabditis briggsiae*, *Schizosaccharomyces pombe*, and *Trichoderma reesei*. These enzymes (Colussi *et al*., 1997; Kruszewska *et al*., 2000) lack the C-terminal hydrophobic region (Figure 1) and require two additional hydrophobic proteins, DPM2 and DPM3, for full activity of a potential three-subunit Dol-P-Man synthase (Maeda *et al*., 1998, 2000; Tomita *et al*., 1998). Due to the significant differences between these two classes of the enzymes, the yeast Dol-P-Man synthase could be considered as a potential target for the development of specific antimicrobial agents that utilize this diversity (Colussi *et al*., 1997). In this respect, studies on the molecular mechanisms of substrate recognition by Dol-P-Man synthases appear essential. Particularly, interactions of the enzymes with the hydrophobic mannose acceptor, Dol-P, and with membranes are expected to differ because of the presence or absence of this terminal hydrophobic sequence.

In this work, we have utilized fluorescence resonance energy transfer (FRET) methodology to obtain useful information on both the structure and the enzyme/substrate interactions of Dol-P-Man synthase. FRET analysis allows measurements of distances between specific amino acid residues in the enzyme and fluorophore/chromophore groups in specially designed substrate analogs. Homogeneous recombinant yeast Dol-P-Man synthase and a truncated form of the enzyme, DPM1Δ3, were expressed in *E. coli* (Schutzbach *et al*., 1993; Zimmerman and Robbins, 1993) and utilized for these studies. DPM1Δ3 lacks 25 C-terminal amino acids including the initially suggested 'dolichol recognition sequence' (Orlean *et al*., 1988), and unlike the full length it contains only one tryptophan amino acid residue, Trp133, and one cysteine residue, Cys93, that is amendable to modification with a chromophoric compound. As such, this truncated enzyme is ideal for fluorescence studies. This sequence was later found not to be essential for activity of the enzyme, and its deletion had little effect on the apparent affinity of the enzyme for Dol-P as judged by K_m values (Schutzbach *et al*., 1993; Zimmerman and Robbins, 1993; Schutzbach, 1994). Several fluorescent analogs of Dol-P with 2-aminopyridine or 1-aminonaphthalene group have been synthesized (Shibaev *et al*., 2000), and our earlier studies favored using the second fluorophore for FRET experiments. The previous studies also established the distance

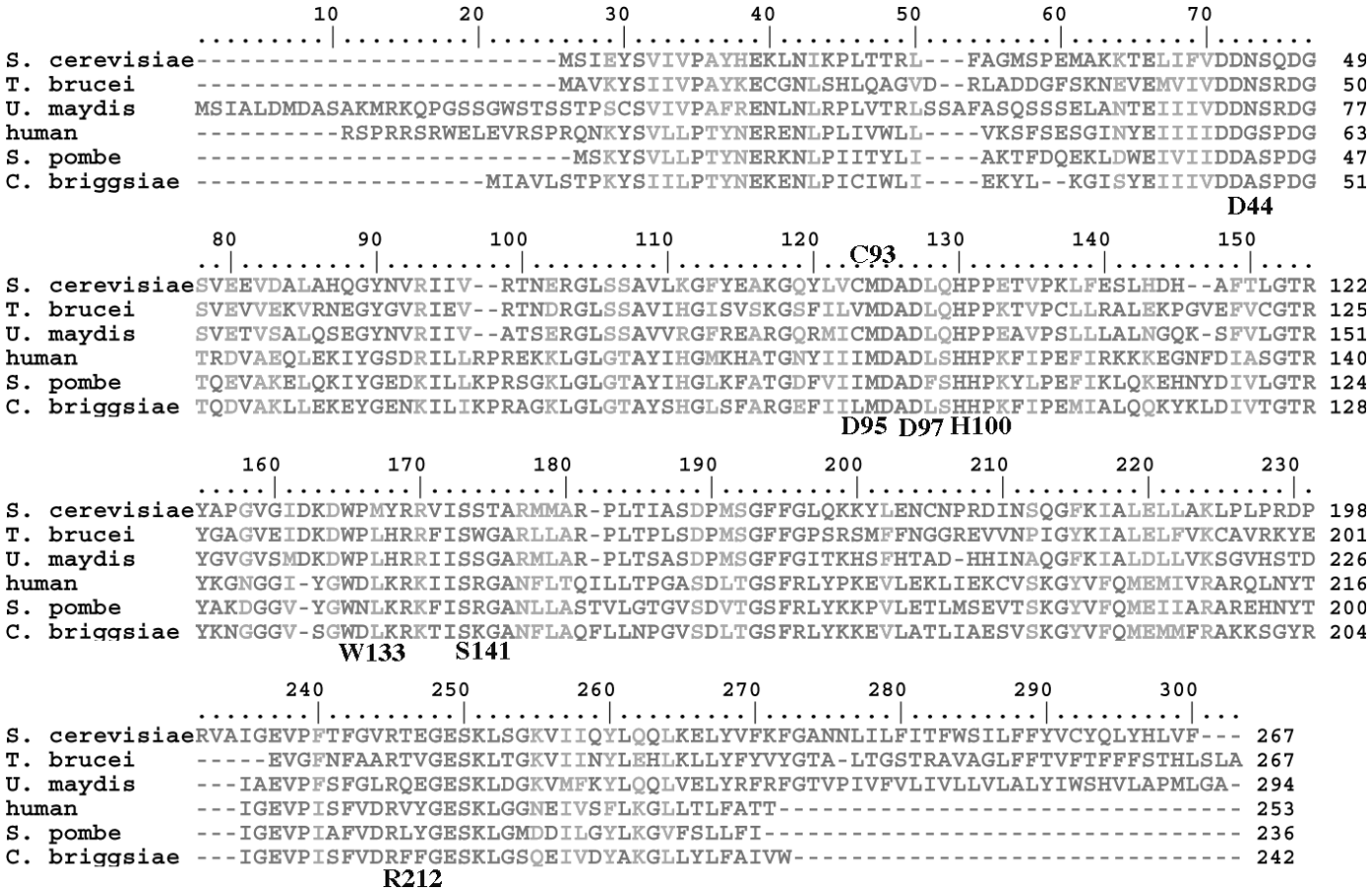

Fig. 1. Sequence alignment of DPM1. The amino acid sequence alignment for Dol-P-Man synthase from *Saccharomyces cerevisiae* (GB_PL1:YSCDPM), *Trypanosoma brucei* (PIR2:S70643), *Ustilago maydis* (GB_PL2:UMU54797), human (SP_HUMAN:015157), *Schizosaccharomyces pombe* (GB_PL1:APAC31G6), and *Caenorhabditis briggsiae* (GB_IN2:AF00787). The *S. cerevisiae* enzyme is 30 amino acid residues longer at the C-terminus than the human DPM1. The C-terminal hydrophobic domain is presumably involved in interactions with endoplasmic reticulum (ER) membranes. Additional labels in black bold typeface refer to selected essential amino acid residues of *S. cerevisiae* DPM1 enzyme as discussed in the text.

between Cys93 and Trp133 in the DPM1Δ3 (Jensen and Schutzbach, 1985; Xing *et al.*, 2000). In this work, we report studies on the interactions of yeast Dol-P-Man synthase with a series of several new 1-aminonaphthalene-labeled dolichols having different distances between the fluorophore and the phosphate group of Dol-P. The FRET experiments allowed for the measurement of distances between selected residues of the enzyme as well as those between the enzyme and chromophoric synthetic Dol-P substrate analogs. State-of-the-art fold recognizing methods were then used to produce a reliable 3D model of the enzyme. The FRET distances were used to evaluate and select the best 3D model for this enzyme with binding of its substrates, GDP-Man and Dol-P.

Results

Synthesis of fluorescent Dol-P analogs

Dol-P-Man synthase is a membrane-bound enzyme that catalyzes reversible transfer from water-soluble GDP-Man to long-chain Dol-Ps found in membranes of the ER. These hydrophobic acceptor substrates have chain lengths ranging from 14 to 17 isoprene units, and although the substrate specificity of the enzyme for GDP-Man is quite high, the enzyme is less specific in regards to specificity for the hydrophobic glycosyl acceptors (Palamarczyk *et al.*, 1980; Lehle *et al.*, 1983; Chojnacki *et al.*, 1984; Jensen and Schutzbach, 1986; Palamarczyk *et al.*, 1987; Wilson *et al.*, 1993; Xing *et al.*, 2000). On the basis of this knowledge, two series of fluorescent Dol-P analogs were designed and synthesized in order to study interactions of yeast Dol-P-Man synthase with different fragments of the dolichol polyisoprene chains. The first set of compounds has a 1-aminonaphthyl fluorescent group at the ω-end of the polyisoprene chain (compounds **1**–**3**) (Figure 2A). Readily available plant polyprenols were used as starting materials for their synthesis. In this series, compound **3** is quite similar in chain length to the main components of yeast dolichols. It is composed of 15 isoprene units (1 dihydro-, 2 *E*-, and 12 *Z*-isoprene units), with two additional carbon atoms remaining from the ω-terminal unit as a result of the synthetic method. In the derivative, the O- and N-atoms are linked through a linear chain of 62 carbon atoms with 15 methyl branches which includes 14 double and 49 single bonds. Derivative **1** is similar in structure but contains only four *Z*-isoprene units (30 carbon atoms in a linear chain with seven methyl branches). Compound **2** is of intermediate chain length (42 carbon atoms in a linear chain with 10 methyl branches) but, due to stereochemistry of the starting plant polyprenol, contains three *E*-isoprene units in the part of the chain close to the fluorophore group. It was expected that in these synthetic substrates, the distances between the fluorophore and the phosphate group, which has to be fixed at the active site of the enzyme, would differ significantly. By comparison, the second set of the analogs (compounds **4** and **5**) was synthesized with the aminonaphthalene residue linked to the former methyl group of the third isoprene unit from the α-end of the chain. These two acceptors thus have equal distances between the fluorophore and the phosphate group (12 carbon atoms in linear chain between the O- and N-atoms with two methyl branches) but differ in the length of the 'tail' of the polyisoprene. Fluorescence excitation and emission spectra of compound **3** in an aqueous environment were reported in our previous manuscript (Xing *et al.*, 2000). Studies of the new synthetic derivatives **1**, **2**, **4**, and **5** demonstrated quite similar spectra, that is, an excitation maximum near 340 nm and the emission maximum near 410 nm (results not shown).

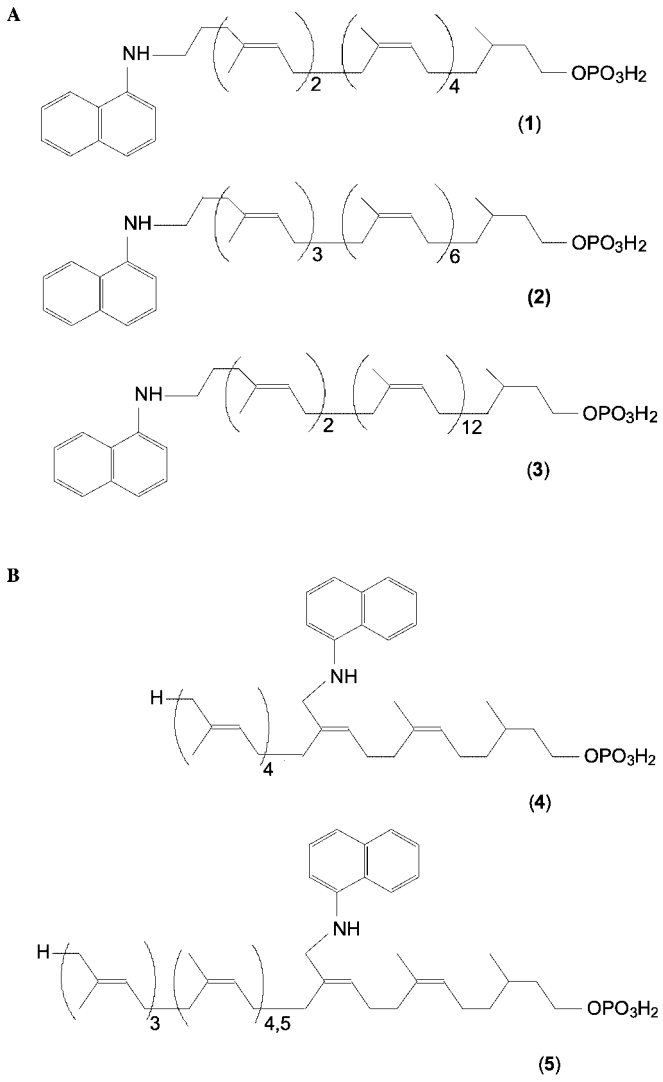

Fig. 2. Chemical structures of fluorescent-labeled synthetic derivatives. All compounds were prepared as diammonium salts. (**A**) Dolichyl-derivatives with fluorophore at the ω-end of the chain: (1) $NafNH(CH_2)_2$-T_2C_4S-*P*; (2) $NafNH(CH_2)_2$-T_3C_6S-*P*; and (3) $NafNH(CH_2)_2$-$T_2C_{12}S$-*P*. (**B**) Dolichyl-derivatives with fluorophore at the γ-position of the chain: (4) $WT_3C(NHNaf)CS$-*P* and (5) $WT_2C_{4\text{-}5}C(NHNaf)CS$-*P*.

Catalytic properties of the substrate analogs

The specificity and affinity of wild-type DPM1 synthase toward the synthetic substrates were assessed in enzyme assays using the biphasic solvent partitioning assay (see experimental procedures). All of the new synthetic polyisoprenoid phosphates (compounds **1**, **2**, and **4**) were substrates for the enzyme with kinetic constants equivalent to natural Dol-Ps (Table I). The kinetic parameters for derivative

Table I. Properties of Dol-P substrate and its fluorescence derivatives with the DPM1 Dol-P-Man synthase

Substrates	Dol-P[c]	1	2	3c	4
K_m (μM)[a]	9.8 (0.8)	24.6 (3)	24.8 (1.1)	11.7 (0.8)	75.1 (4)
k_{cat} (U/mg)[a,b]	17.6 (0.5)	18.4 (0.7)	20.1 (0.3)	22.4 (1.2)	18.8 (0.4)

Compounds **1**–**4** are as defined in Figure 2 and in the text.
[a]Kinetic parameters, K_m and k_{cat}, were determined by non-linear regression methods using the computer programs EZ-FIT and ENZFIT (Elsevier-Biosoft). Compound **5** (see Figure 2) was not included due to its similarity to compound **4**, which resulted in similar kinetic properties (data not shown). Errors of measured K_m and k_{cat} values are reported in parenthesis.
[b]One unit of enzyme activity, 1 U, was defined as 1 μmol of mannose transferred from GDP-Man to polyprenyl-P per min per mg of enzyme.
[c]Data from reference (Xing *et al*., 2000).

3 were reported in our previous study (Xing *et al*., 2000). Values of k_{cat} are essentially identical for all the derivatives studied (18.4–22.4 U/mg) and equivalent to k_{cat} for Dol-P (17.6 U/mg). The differences in apparent affinity of the enzyme for the various substrates, as judged by K_m values, are small and probably not significant. The data therefore suggest that the optimal geometry of catalytic groups in the active site is retained, even with substrates having significantly diminished chain length as compared with Dol-P. In addition, as the catalysis proceeds similarly to that with the Dol-P substrate, it therefore appears that the analogs affect the GDP-Man-binding affinity.

Distances determined by FRET measurements and utilization of C55-P structure

Fluorescence measurements were carried out utilizing the truncated but active form of the enzyme, DPM1Δ3, which has a deletion of the 29 C-terminal amino acid residues. This sequence includes the putative transmembrane segment of the synthase but is not required for activity or for interactions with Dol-P *in vitro*. The distances between the Trp133 residue of DPM1Δ3 and the fluorophore on compounds **1**–**5** (Figure 2) were determined using FRET analysis (Figure 3). In addition, the distances between the Cys93 residue labeled with a 4-dimethylaminophenylazophenyl-4′-maleimide (DAMBI) chromophore and compounds **1** and **3a** were also determined (Table II, Figures 2 and 3). Compound **3a** for all practical purposes is identical to compound **3** except it is a mixture of Dol-P analogs having 13–15 isoprene units, with 14 being the predominant one. Our earlier studies on both compounds **3** and **3a** exhibited the same distance values (Xing *et al*., 2000). The calculated distances between all fluorescent residues range from the shortest of 15.3 Å from compound **1** to Trp133 and the longest distance of 35.5 Å from compound **3a** to Cys93-DAMBI.

The FRET measurements were supplemented by the published distances measured directly from the structure of undecaprenyl phosphate C55-P, a Dol-P analog, obtained by nuclear magnetic resonance (NMR) and molecular modeling (Zhou and Troy, 2003). This structure allowed for approximation of the distances between the phosphate group and various sites of attachment of fluorescent groups in the synthetic substrate analogs.

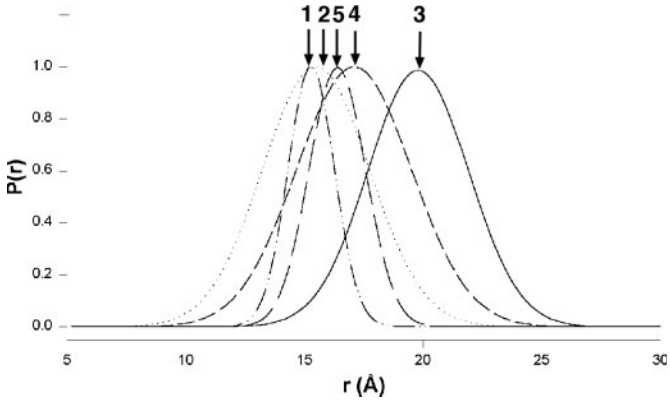

Fig. 3. The distribution of the distances between Trp133 and synthetic chromophoric substrate for the DPM1Δ3 mutant of Dol-P-Man synthase. The donor was Trp133 and the acceptor was the dolichyl-modified substrates. The distribution was determined in the presence of a 10-fold excess of the substrates and were peak-normalized to facilitate comparison: p(r) probability of distance r (Å) for compounds **1** through **5**: **1** –.. ; **2** ... ; **3** — ; 4 – – ; 5 — — (also labeled by compound number above the curves).

Table II. Distance parameters for Dol-P-Man synthase[a]

Distance	R_o (Å)	r (Å)	hw (Å)	3D model[d] (Å)
Trp133–Cys93, no substrate[b]	21.2	22.3[c]	5.0[c]	19
Trp133–Cys93, with Dol-P[b]	21.2	19.0	4.1	19
Trp133–compound **1**, fluorophore	17.8	15.3	2.3	12
Trp133–compound **2**, fluorophore	18.0	15.5	5.3	18
Trp133–compound **3**, fluorophore	20.3	19.8	5.0	NA[e]
Trp133–compound **4**, fluorophore	19.3	17.1	5.7	14
Trp133–compound **5**, fluorophore	17.8	16.4	2.8	14
Cys93–compound **1**, fluorophore	41.0	29.4	5.6	24
Cys93–compound **3a**[f] fluorophore[b]	41.4	35.5	6.3	NA[e]

[a]These results were obtained with mutant enzyme DPM1Δ3.
[b]These distances are taken from (Xing *et al*., 2000) and are given here for ready comparison with the present results.
[c]The half-width of a given distribution (hw) is related to the standard deviation (σ) of the distribution by $hw = 2.345\sigma$. The goodness of the distribution fits was evaluated by the reduced χ^2 values (not shown). The uncertainties of the mean distance (r) and hw were assessed by the uncertainties associated with an increase in the normalized reduced χ^2 value of one standard deviation (F-statistic), and these uncertainties define the possible errors associated with the determination of the parameters from the distance distribution. The uncertainties of the reported values of r are in the range 0.1–0.4 Å, and those of hw are also in the range 0.1–0.4 Å.
[d]Distances within the model of the DPM1-substrates complex were measured between Sγ of Cys93 or CE2 of Trp133 and the carbon of the CH3 group of the isoprene unit to which the chromophore of Dol-P, 1-aminonaphthalene, is attached. Such distances are only approximation of spacing between chromophores and are reported with only two significant figures.
[e]NA—distance not available due to the length of Dol-P extending beyond the length of available Dol-P model coordinates.
[f]Compound **3a** is a mixture of oligomer-homologs where the number of isoprene units varies from 12 to 15 with an average of 14 units (Xing *et al*., 2000), as for single species compound **3**.

3D homology modeling of S. cerevisiae *DPM1 structure*

In order to elucidate the structural model of the DPM1 enzyme, sensitive fold recognition analyses were performed primarily using the META server (http://bioinfo.pl/Meta) (Bujnicki *et al.*, 2001). The rationale for obtaining a model was to visualize the structure of the protein and its interactions with substrates and product and to possibly explore the catalytic mechanism and the potential amino acid residues involved in catalysis. All methods employed at the META server indicated consistently that DPM1 synthases from all sources, including that from *S. cerevisiae*, were similar to one another at the primary, secondary, and tertiary levels and that all DPM1 synthases were similar in fold to the structure of the spore coat polysaccharide biosynthesis protein A (SpsA) glycosyltransferase (GT) for which a 3D X-ray structure has been elucidated (protein data bank [pdb] code: 1h7l) (Tarbouriech *et al.*, 2001).

For modeling, we chose to utilize the methodology implemented by the Robetta structure prediction server (Chivian *et al.*, 2003a). All model structures, including Robetta homology/comparative models, must be viewed with caution, as compared with experimental structures obtained using either X-ray crystallography or NMR. However, we had experimental data available, primarily the FRET distances that allowed for critical evaluation of all the models produced and selection of the best model. The structural models produced by the Robetta server were first evaluated using objective protein quality measures as implemented in PROSA II (Sippl, 1993), VERIFY_3D (Eisenberg *et al.*, 1997), and ProQ (Wallner and Elofsson, 2003). The bases for these quality analyses were largely independent of those contained within the Robetta structure prediction and therefore were suited to identify the best, correct model out of the five models provided. Two of the models produced by Robetta performed best by all three methods ProQ, PROSA II, and VERIFY_3D. However, utilization of FRET data, primarily the distance between Cys93 and Trp133, allowed for a clear identification of the one correct model.

Similarly to SpsA GT, a two-domain structure was predicted for DPM1 enzyme. The N-terminal domain, nucleotide-binding in SpsA, consists of parallel β-strands flanked on both sides by α-helices (Figure 4A). The C-terminal domain consists of antiparallel β-strands, also with helices on both sides (Figure 4A). This domain in SpsA is a sugar acceptor. The C-terminal half of the C-terminal domain is significantly more hydrophobic than the remaining parts of the enzyme suggesting association with the ER membranes and with the Dol-P substrate (Figure 4C and D).

The identification and structural properties of the DPM1 active site

The 3D structure of SpsA complex with deoxythymidine 5′-diphosphate (dTDP) and either Mg^{2+} or Mn^{2+} (Tarbouriech *et al.*, 2001) has permitted the identification of the active site in the analogous DPM1 model. Comparison of the structural alignment of SpsA with the DPM1 model allowed the substrate GDP-Man molecule to be relatively precisely placed in the active site. Along with GDP-Man, two Mg^{2+} ions were also placed in the active site based on structural alignments with the SpsA complex (Figure 4). In addition, the availability of the structure of the C55-P analog of Dol-P allowed for positioning of the hydrophobic substrate in the DPM1 active site. The positioning of the substrates took into account geometric restrictions and the possibility to interact with hydrophobic parts of the enzyme. Utilization of the FRET distance data (Table II) facilitated and corroborated this process (Figure 4B).

Discussion

Natural dolichols and substrate properties of fluorescent Dol-P analogs

Yeast Dol-P-Man synthase is found in membranes of the ER, where it is involved in the reversible formation of Dol-P-Man, a key intermediate in glycoconjugate biosynthesis (Kinoshita *et al.*, 1997, Schutzbach, 1997; Drickamer and Taylor, 1998; Ferguson, 1999; Schenk *et al.*, 2001). The dolichols comprise a family of long-chain polyisoprene alcohols having the general structure $WT_2C_{n-4}S$-OH (IUPAC-IUB recommendations on nomenclature). The molecules have one dihydroisoprene unit at the α-end of the polyisoprene chain and two isoprene units in the *E*-(*trans*-) configuration at the ω-end, with the remainder of the chain composed of *Z*-(*cis*-) isoprene units. Natural dolichols are usually found as species-specific mixtures of similar chain-length polyisoprenes in any particular organism (Shibaev, 1997; Schenk *et al.*, 2001). Thus, dolichols isolated from mammalian cells contain 18–21 isoprene units (C_{90}–C_{105}), whereas yeast dolichols are composed of 14–17 isoprene units (C_{70}–C_{85}) with dolichol-15 (C_{75}) and dolichol-16 (C_{80}) being the main components. Dolichols have been reported to have somewhat coiled structure with an average raise of the coil of ~2.6 Å with the diameter of each coil of 5.8 Å. Both termini of dolichols have more elaborate structures than that of a coil (Murgolo *et al.*, 1989; Zhou and Troy, 2003, 2005). The structures of our derivative dolichyl-like compounds are assumed to be similar to that of dolichol because interactions with the enzyme are similar based on the kinetic constants.

We have previously demonstrated that yeast Dol-P-Man synthase can utilize both natural and chemically modified full-length dolichols as mannosyl acceptors with almost equal efficiency (Xing *et al.*, 2000). Shortening the poly-*cis*-fragment by five or eight *C*-isoprene units as in derivatives **1** and **2** results only in an approximate 2-fold increase of K_m values (Table I), suggesting that the main contribution to the enzyme–substrate interactions is due to the C_4S-P fragment of the Dol-P molecule. By comparison, modification of the γ-isoprene unit is less favorable for the enzyme–substrate interactions because the K_m for derivative **4** is 3- to 7-fold higher than that for Dol-P or derivatives **1**, **2**, and **3**. On the basis of our earlier studies, the much shorter and water-soluble derivative $PyNH(CH2)_2$-CS-*P* (Xing *et al.*, 2000) was a very inefficient in binding to the enzyme (K_i was ~200 times higher than the K_m value for the natural substrate Dol-P), but this structure appears to represent the

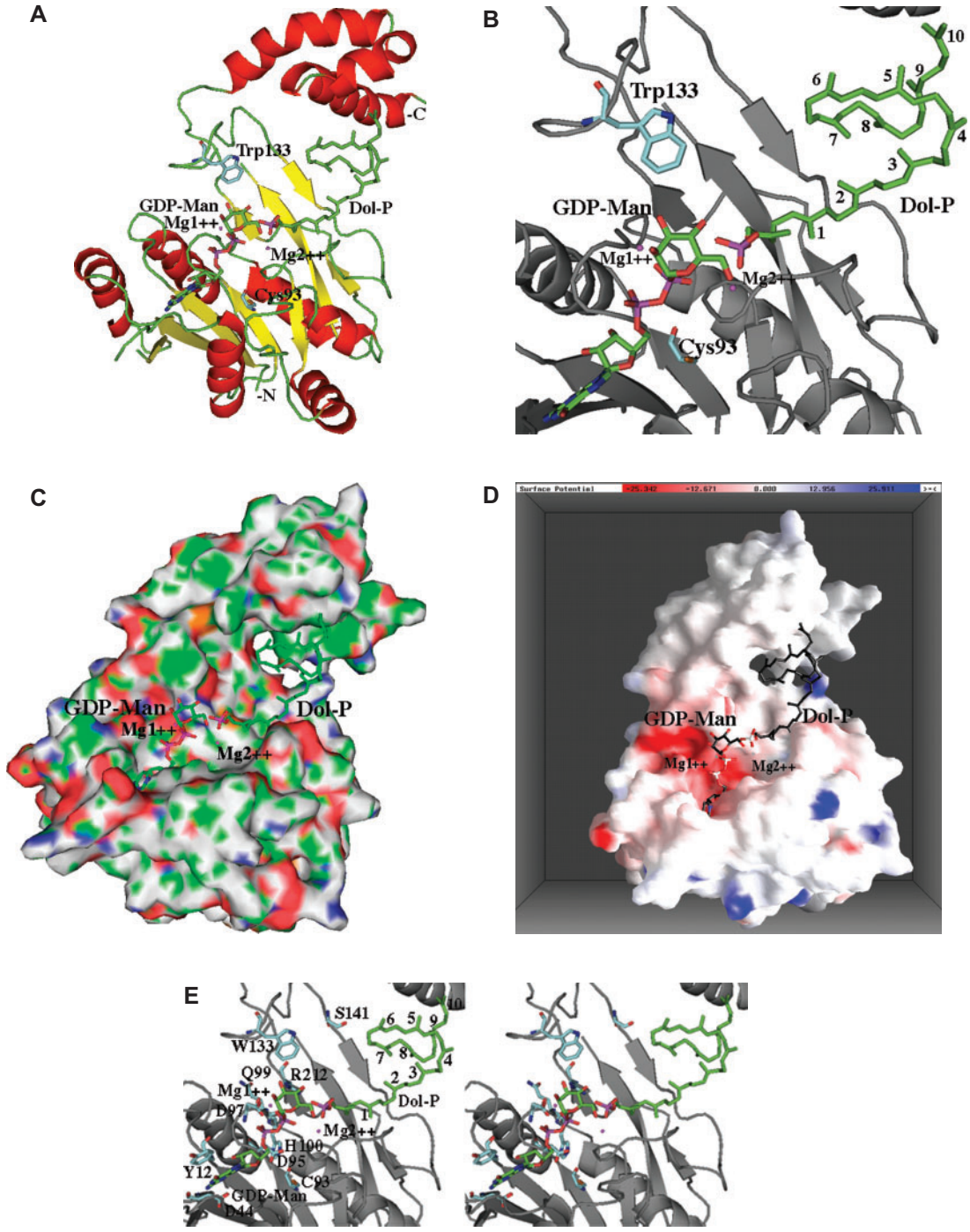

Fig. 4. Three-dimensional (3D) structural model of *Saccharomyces cerevisiae* Dol-P-Man synthase. The model for the catalytic domain of Dol-P-Man synthase was obtained using the Robetta server (Chivian *et al*., 2003b) and was based on comparative/homology modeling utilizing the structure of glycosyltransferase SpsA (pdb code: 1h7l) (Tarbouriech *et al*., 2001). The figure demonstrates a characteristic fold of this two-domain protein, with the N-terminal domain supporting nucleotide binding of GDP-Man and the C-terminal domain binding Man (of GDP-Man) and Dol-P. All panels **A**–**E** represent the molecule and substrates in the same orientation. (**A**) 3D model of DPM1. The molecule is color-coded by the secondary structure elements (helices in red, β-sheets in yellow, other in green). The bound GDP-Man and Dol-P molecules are located in the substrate-binding cleft and are depicted in ball and stick fashion colored by atom type (C, green; N, blue; O, red; P, pink; S, yellow). The N-terminal and the C-terminal domains are depicted; the termini are labeled. (**B**) Active center of DPM1. Both substrates, GDP-Man and Dol-P, two putative Mg^{2+} ions, and two chromophoric residues of the enzyme Cys93 and Trp133 appear as blue balls and sticks (colored by atom type). The consecutive isoprene units of Dol-P are labeled. (**C**) Surface of the DPM1 molecule and both substrates bound in the cleft. The protein surface is colored by the atomic element (C, green; N, blue; O, red; S, yellow). The substrates are colored as in panel **A**. (**D**) DPM1 surface colored by electrostatic potential. The hydrophobic character of the C-terminal region suggests its membrane interactions/insertion. (**E**) Wall-eyed stereo view of the active cleft of the DPM1 complex. The amino acid residues implicated in the binding of substrates, catalysis and functional properties of the enzyme are rendered in a ball and stick fashion (selected amino acids of the enzyme are depicted with blue bonds, substrates' bonds are in green, atoms are color-coded by type). The consecutive isoprene units of Dol-P are labeled as in panel **B**. The substrates and Mg^{2+} ions are depicted similarly as in panel **B**.

shortest fragment that occupies the active site. The CCS-P fragment is thus the minimal part of the molecule necessary for the binding to the enzyme.

FRET-based distance measurements

Although recombinant yeast Dol-P-Man synthase can be purified to homogeneity in relatively large quantities (Zimmerman and Robbins, 1993), all attempts to crystallize the protein for subsequent 3D structure determination have proven negative, presumably due to the hydrophobic nature of the protein. DPM1, however, has several unique features that allow the use of FRET analysis to measure specific atomic distances within the protein as well as with bound substrates labeled with fluorescent chromophores. Both DPM1 and the C-terminal truncate, DPM1Δ3, are fully active enzymes and bind the two substrates GDP-Man and Dol-P with equal affinity. Both enzymes contain only one reactive Cys residue, Cys93, that can be readily derivatized (Jensen and Schutzbach, 1985; Saxena *et al.*, 1995), and in DPM1Δ3, there is only a single Trp residue, Trp133, that is useful for fluorescence studies. Cys93 in both forms of the enzyme was labeled with DAMBI and a series of Dol-P analogs was synthesized, labeled with the fluorescent probe 1-aminonaphthalene. In our earlier studies, we utilized 2-aminopyridyl labeled Dol-P analogs and in those studies labeled Cys93 with (5-iodoacetamidoethyl)aminonaphthalene-1-sulfonic acid (1,5-IAEDANS) (Xing *et al.*, 2000). The 1,5-IAEDANS-labeled enzyme was utilized primarily for measuring distances between Cys93 and Trp133 as reported (Xing *et al.*, 2000), but the 2-aminopyridine probe was found inadequate for the current studies because of the overlap of its spectral properties with those of the Trp133 residue.

In the current studies, we have relied on the triangulation of various FRET distances measured point-to-point within the protein and between specific amino acid residues in the protein and the fluorescent Dol-P analogs to delineate the structural properties of DPM1 and its active site location. This type of analysis provides a wealth of information regarding the enzyme but is more limited in scope as compared with the information obtained from a 3D structure. The FRET data for compounds **1**–**5** and the enzyme are summarized in Table II. For comparison, we have also included in Table II four additional distances, which were previously reported (Xing *et al.*, 2000). It should be noted that the half-width of all distributions are within the range 2–6 Å, which are relatively narrow distributions. The binding of substrate results in a small narrowing of the distribution suggesting a slightly more constrained Trp133-Cys93 segment.

The distances measured from any of the compounds **1**, **2**, and **3**, which have the fluorophore placed at the ω-terminus of the polyisoprene chain, and Trp133 are in direct relation to the length of the polyprenyl chain. The longest distance is found between Trp133 and the fluorophore on compound **3** (19.8 Å). As the number of isoprene units is decreased to nine in compound **2**, the distance from Trp133 to the fluorophore is ~15 Å (15.5 Å), which is very similar to distance to the fluorophore of compound **1** of 15.3 Å, which is only six polyisoprene units in length. The distance and angular analyses suggest that the chromophores of compounds **1** and **2** are approximately on the same side of the closest point of the dolichol-binding site to Trp133. However, the probes appear to lie in different planes with the fluorophore of compound **1** closer to the catalytic center than compound **2**.

The two measured distances available between the fluorophores of compounds **1** and **3a** (Xing *et al.*, 2000) to DAMBI modified Cys93 are significantly longer than the distances to the enzyme's natural chromophore, Trp133. On the basis of our earlier work, compounds **3** and **3a** provide essentially identical distances from the chromophore to both Trp133 and Cys93-DAMBI, although compound **3a** is an inhomogeneous form with respect to the number of polyisoprene units. The analysis of the distances among Cys93-DAMBI, Trp133, and the fluorophore of either compound **3a** or **3** indicates that the positions of these groups are nearly collinear. Thus, the distance between the Dol-P ω-localized fluorophore and Cys93-DAMBI of 35.5 Å is approximately equal to the sum of the distance between the substrate and Trp133 of 19.8 Å plus the Trp133 to Cys93-DAMBI distance of 19.0 Å, a distance of 37.6 Å (Table II). The approximate length of compound **3**, based on the average of the polyisoprene coil of 2.6 Å per isoprene, is 36.4 Å (Murgolo *et al.*, 1989; Zhou and Shan, 2001; Zhou and Troy, 2005). This distance is in close agreement with the fluorophore to Cys93-DAMBI distance of 35.5 Å, which is consistent with the phosphate group of this compound being placed in the proximity of Cys93 near the catalytic center (Saxena *et al.*, 1995).

The distances from the fluorophore on compound **1** to Trp133 is 15.3 Å and to Cys93-DAMBI is 29.4 Å. This compound is eight isoprene units shorter than compound **3** (or **3a**), and therefore, the fluorophore at the ω-terminus is also closer to the active center of the enzyme. Detailed geometric analysis suggests that the phosphate group of the dolichyl-like substrates is not exactly at the location of Cys93-DAMBI, but rather at a small distance from it.

Summarizing the triangulation distances with the short-chain derivative **1** and comparison with the results of similar triangulation with the long-chain derivative **3** allow the conclusion that (i) for both substrates the fluorophores lie on the same side of the protein from Trp133 and (ii) the distances between Cys93 and the ω-fluorophores (29.4 Å and 35.5 Å for **1** and **3**, respectively) do not change significantly for these two derivatives. The experimentally NMR-derived (Zhou and Troy, 2003, 2005) and computational conformational information available regarding Dol and Dol-P (or their analogs) structures (Murgolo *et al.*, 1989) clearly illustrates that parts A (S-unit) and C (WT2-units) are close to the direction of the Cys93-fluorophore vectors, whereas the spiral part B of the molecule, that is composed of C-units, is almost perpendicular to this vector (Figure 4). Therefore, the elongation of the polyisoprene chain by eight isoprene units does not lead to a large change in the Cys93-fluorophore vector.

By comparison, the FRET distances for derivatives **4** and **5**, which have the fluorescent group localized one isoprene unit away from the saturated α-isoprene unit, indicate that the fluorophore on these substrates is probably situated between Cys93 and Trp133. Compounds **4** and **5**, as

expected, have similar distances from their fluorophores to Trp133. In these analyses, we have assumed that the phosphorylated α-end of Dol-P and the substrate analogs always bind in the same configuration at the binding site that is the catalytic center of the enzyme. Such placement is justified by necessity, which in turn allows for the catalysis to proceed as is reflected in catalytic properties summarized in Table I.

Experimental evidence for the location of the active site of the enzyme

Our current biochemical evidence, based on the use of amino-acid-specific reagents and site-directed mutagenesis, demonstrated that both Cys93 (Forsee *et al*., 1997) and His100 (Jensen and Schutzbach, 1985) are important for activity and suggested that they are in proximity to the active site of the enzyme. In addition, sequence and hydrophobic cluster analysis carried out by Colussi *et al*. (1997), who suggested the possibility that Asp44 and Asp95 might participate in catalysis (Saxena *et al*., 1995; Colussi *et al*., 1997). The Asp95 residue is quite close in sequence and, therefore, in 3D structure to Cys93 as well as to His100. In addition, the stretch of residues including Met94-Asp95-Ala96-Asp97, followed by His100, and Pro102 (Figure 1) are strictly conserved in all Dol-P-Man synthases known to date. This strict conservation may reflect the catalytic importance of these residues. Other strictly conserved residues that presumably bind and position the GDP-Man substrate for catalysis (Figures 1 and 4B, E) include Asp44, Trp133, Ser141, and Arg212. The Ser141 amino acid residue has been implicated as a site for phosphorylation and has been proposed to regulate activity (Banerjee *et al*., 2005).

There are two substrate analogs, **1** and **3/3a**, for which distances from their ω-localized chromophores to both Cys93 and Trp133 have been established. The distances measured between the ω-terminal 1-aminonaphthyl fluorescent group of derivative **1**, with six isoprene units, and Cys93 or Trp133 were 29.4 Å and 15.3 Å, respectively. Our earlier fluorescence studies carried out with derivatives **3**, having 14 isoprene units, and its analog with 12–15 isoprene units (compound **3a**, 14 isoprene units on average), demonstrated that these two compounds bind at the same site. The FRET distances from the ω-terminal 1-aminonaphthalene chromophores in compounds **3** and **3a** to Cys93 and to Trp133 of DPM1Δ3 were 35.5 Å and 19.8 Å, respectively (Table II). In addition, our previous results demonstrated that the Trp133–Cys93 distance in DPM1 is 19.0 ± 0.2 Å in the presence of the Dol-P substrate and 22.3 ± 0.1 Å for the apoenzyme form (Table II). On the basis of the structure of C55 Dol-P (Zhou and Troy, 2003), the distance between phosphate of Dol-P and the CH_3 carbon of the seventh isoprene unit is ~14 Å. By simply extending the C55 Dol-P chain by additional isoprene units (to achieve a total of 14 isoprene units), the distance between P and the ω-isoprene's CH_3 would be ~25 Å. Considering both cases involving compounds **1** and **3/3a**, simple triangulation calculations place the phosphate group of Dol-P, and the center of the catalytic site of the enzyme, somewhere between Cys93 and Trp133. Because both compounds are catalytically active (though to different degrees), the binding of Dol-P and its analogs (phosphate group and near isoprene units) at the catalytic site are assumed to be similar.

3D model of DPM1

In the absence of crystal structure data, state-of-the-art methodology was used for the construction of a 3D analogy model of DPM1 based on the known structure for the GT SpsA along with its complex with dTDP and Mg^{2+} ions (Figure 4). The DPM1 structure was validated by agreement with intramolecular distances based on the FRET analysis. The model allowed the positioning of C55-P in the DPM1 active cleft along with construction of a full model exhibiting the DPM1–GDP-Man–Dol-P complex. The model also permits: (i) the identification of two domains in the protein with specific functions, nucleotide- and glycosyl/Dol-P- binding sites; (ii) identification of the active site cleft along with residues previously identified in the site with the use of amino-acid-specific reagents and site-directed mutagenesis, and those residues that are highly conserved among species (Figure 1); (iii) identification of hydrophobic C-terminal regions involved in binding Dol-P and potentially involved in interaction with ER membranes; (iv) visualization and rationalization of the FRET distance data; (v) identification of the potential catalytic site; and (vi) the rationale for the absolute requirement of divalent cations for activity. The model of the full complex also allows measurements of approximate distances in the model corresponding to FRET distances measured in the enzyme and summarized in Table II and shown Figure 4B. Thus, the Cys93 to Trp133 distance of 19 Å in the model corresponds to the 19.0 Å FRET distance measured in the enzyme with bound Dol-P (Table II and Figure 4). This agreement of the distance data is striking and further supports the accuracy of the model.

The model illustrates the active site as a long, shallow, and wide cleft spanning two domains of the protein. Its GDP-binding site is confined to the N-terminal domain, whereas Man and Dol-P are restricted to the C-terminal domain (Figure 4). The electrostatic properties identified in the active site are ideally suited for interactions with the two substrates. The site involves both a highly charged surface environment in the nucleotide and sugar-binding part of active site cleft, with primarily neutrally charged and hydrophobic residues in the dolichol-binding domain (Figure 4C and D). The polyisoprene hydrophobic tail of Dol-P interacts with the C-terminal half of the domain that appears to allow for a significant degree of flexibility. In contrast, GDP-Man is relatively rigid in its binding site. The major binding interactions of the enzyme with Dol-P are restricted to a few isoprene units and the phosphate at the α-terminus of the molecule. This was already suggested by the catalytic data (Table I) demonstrating that the apparent K_m values of the acceptor substrates are similar for both short-chain and long-chain polyisoprenes and thus less dependent upon the ω-end of the chain.

Of significant interest is also the role of the hydrophobic domain of the enzyme. Although residues beyond Phe239 can be deleted with little or no effects on enzyme activity

in vitro, the model demonstrates that these residues are associated with the ω-terminus of the Dol-P and as such are likely to be involved in the direct interactions with the ER membrane, the phospholipids bilayer, where Dol-P is presumably stored. As such, this domain might be involved in Dol-P recognition and transport to the active site of the enzyme. The analysis of the surface properties of this region of the DPM1 protein molecule suggests that it could be involved in such interactions (Figure 4C and D). Specifically, the C-terminal region of DPM1 model with higher hydrophobic character, the gray-colored part depicted in Figure 4B, which is composed of three semi-parallel α-helices (Figure 4A), appears to be consistent with its involvement in membrane interactions. However, the experimental evidence in support of such conclusion is still lacking.

Active site and the mechanism of action

Analysis of the catalytic site containing the two bound substrates allows the identification of amino acid residues potentially involved in substrate binding and catalysis. Our model demonstrates that Tyr12 and Asp44 interact with the guanine group of the GDP segment. Although this location appears distant from where catalysis might occur, Tyr12 and Asp44 appear to take part in binding and positioning the GDP moiety of the substrate. These interactions were also implicated in providing specificity for the selection of sugar donor (Tarbouriech *et al.*, 2001), GDP-Man. The commonly recognized DxD motif of GTs consists from Asp95xAsp97 (where x is any amino acid residue) (Figure 4E). The Asp95 amino acid residue does not participate in direct interactions with the GDP-Man substrate in our model. However, Asp97 interacts with one of the Mg^{2+} ions (OD2–$Mg1^{2+}$), and the same $Mg1^{2+}$ interacts with oxygen ions of both phosphate groups of GDP-Man (Figure 4E). As such, the DxD motif in Dol-P-Man synthase appears to position the catalytic end of the glycosyl donor, GDP-Man, for the transfer reaction of the mannosyl residue to Dol-P. On the basis of structural alignments, the catalytic base in SpsA protein, Asp191 that facilitates SpsA catalysis by activating acceptor's hydroxylate, does not have a corresponding residue in Dol-P-Man synthase, as this region of the enzyme is a portion of the alignment gap. Such behavior clearly suggests a modified mechanism to this enzyme. As the acceptor molecule is not a sugar molecule, but Dol-P, there is no hydroxyl group to activate for nucleophilic attack. The oxygen of the Dol-P phosphate group is already activated for nucleophilic attack. The active site of the Dol-P-Man synthase enzyme facilitates such nucleophilic attack by bringing the catalytic portion Dol-P phosphate close to the C1 carbon of mannosyl residue. Coincidentally, Arg212 in the Dol-P-Man synthase model interacts with specific positions on both the mannosyl moiety of GDP-Man (NH1 of Arg212 with O3) and the oxygen ion of the phosphate group of Dol-P (NH2 of Arg212 with O4). In addition to Arg212, the $Mg2^{2+}$ ion also interacts with the oxygen ions of two phosphate groups but from two substrates GDP-Man (terminal phosphate) and Dol-P (Figure 4E), indicating that the divalent cations, presumably both of them $Mg1^{2+}$ and $Mg2^{2+}$, are required to present the phosphate residues in the proper configuration at the active site for

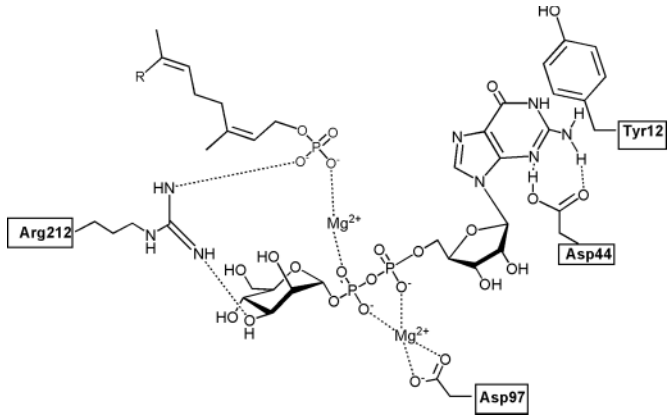

Fig. 5. Single displacement inverting mechanism for Dol-P-Man synthase. This mechanism of Dol-P-Man synthase involves a single displacement mechanism with the inversion of configuration at C1 of the mannosyl residue. It proceeds through an intermediate reaction step involving an oxocarbenium ion at the C1 position of the mannosyl moiety. The nucleophile/base function is performed by one of the activated oxygen of the Dol-P phosphate group.

mannosyl transfer. As such, Dol-P-Man synthase is a presumed binuclear metalloenzyme utilizing magnesium in its catalytic process (Jedrzejas and Setlow, 2001) (Figure 5).

This mechanism of Dol-P-Man synthase is, therefore, a modified form of inverting GT-2 GTs and involves a single displacement mechanism with the inversion of configuration at C1 of the mannosyl residue. The catalytic process is thought to proceed through an intermediate reaction step involving an oxocarbenium ion at the C1 position of the mannosyl moiety. The nucleophile/base function is performed by one of the activated oxygen of the Dol-P phosphate group (Figure 5). However, it must be remembered that Dol-P-Man synthase catalyzes the reversible formation of a high-energy product that can further serve as a glycosyl donor. Therefore, the exact mechanism may differ slightly and can only be established with more accurate studies of the active site as provided by experimental structure or further site-directed mutagenesis.

Conclusions

In summary, in the absence of an experimental 3D structure for Dol-P-Man synthase determined by either crystal X-ray diffraction or NMR, fluorescence techniques were utilized to elucidate structural properties of the enzyme. A single natural Trp residue and a single modified Cys residue in the mutant enzyme, DPM1Δ3, were used as markers to measure distances from the amino acid residues to an aminonaphthyl group present on several different synthetically modified dolichyl derivatives. These derivatives were all substrates for the enzyme. The fluorescence methodology used in the studies allowed for the triangulation of distances between Trp133, modified Cys93, and the fluorescent probes of the dolichyl-derived compounds. Such distances in turn were used in delineating selected structural properties of the enzyme's active site and its dolichyl-binding pocket. The available structure of SpsA allowed the

creation of an analogous 3D model for DPM1 that agrees nearly perfectly with the experimental data available, including the FRET-derived distances. The model structure allowed for the identification of the active site cleft, its properties, and a putative functional mechanism.

It is very unfortunate that SpsA is still a molecule of unknown specificity as it is the only known example of the very voluminous family 2 of inverting GTs with known crystal structure. Similarly to the SpsA, DPM1 synthase belongs to the family 2 of GTs (GT-2). DPM1 is the first GT molecule with 3D structural information available (this study) that utilizes GDP-sugar as a substrate (as opposed to uridine 5′-diphosphate (UDP)-sugars). In addition, DPM1 is novel as it is the first molecule where phosphate group (not hydroxyl group) is subjected to glycosylation in the acceptor molecule. Such enzymes have not been investigated structurally before. The family 2 of inverting transferases, to which DPM1 belongs, is the largest and most widespread group among GT enzymes. Within this family, the amino terminal domains usually exhibit a degree of structural homology, whereas the C-terminal domains have a large diversity of structural and functional properties. Due to this diversity, this domain is suited to utilize a large number of different glycan and other structures as acceptors. One of these variations allows for binding Man (from GDP-Man) and Dol-P. Due to the hydrophobic character of Dol-P, this domain's surface in the DPM1 enzyme is lined with hydrophobic residues and the hydrophobic C-terminal sequence may interact with ER membranes, where Dol-P is located along with the Dol-P-Man product of the reaction. This product is further utilized by other GT enzymes for the specific glycosylation of proteins.

Materials and methods

Enzyme purification and assay

The full-length (DPM1) and the truncated version of the Dol-P-Man synthase, containing residues 1–238 of the full-length enzyme (DPM1Δ3), were expressed in *E. coli* and purified as previously described (Schutzbach *et al*., 1993; Xing *et al*., 2000). The purified enzyme was dialyzed against 10 mM tris(hydroxymethyl)aminomethane (Tris)–HCl buffer (pH 7.5), 0.15 M NaCl, 1 mM dithiothreitol (DTT), and 0.2% Nonidet P40 (ethylphenylpolyethyleneglycol) (NP-40) and concentrated using a WM-10 membrane (Amicon) to 2 mg/ml. Protein concentration was determined using UV absorption at 280 nm based on the enzyme's calculated extinction coefficient (Pace *et al*., 1995). All procedures were performed in a cold-room at 0–4°C or at ice bath temperature.

The enzyme assay was based on the differential partitioning of the radioactive substrate, GDP-[^{3}H]Man, and products in a two-phase scintillation mixture as previously described (Jensen and Schutzbach, 1985; Xing *et al*., 2000). One unit of enzyme activity was defined as 1 μmol of mannose transferred from GDP-Man to the natural or synthetic substrates per minute and per milligram of enzyme. Kinetic parameters of the enzyme with various substrates were calculated using non-linear regression computer programs as described (Schutzbach *et al*., 1993; Xing *et al*., 2000). The k_{cat} parameter was used, and not V_{max}, as it is a turnover number and allows for the comparison of enzymes of different sizes.

Synthesis of fluorescent-labeled Dol-P derivatives

Dol-P derivatives with fluorescent label at the ω-end of the chain **1**–**3** (Figure 2A) were synthesized from (±)-dolichols prepared from readily available plant polyprenols (Veselovsky, 1999; Veselovsky and Lozanova, 2000). Polyprenols from pine needles were used as starting material for the synthesis of **3** (Shibaev *et al*., 2000; Veselovsky *et al*., 2001a). In brief, the synthetic procedure included selective van Tamelen epoxidation of the ω-terminal isoprene unit in dolichyl acetates (Shibaev *et al*., 2000; Veselovsky *et al*., 2001a), HPLC separation of the resulting epoxides, and the conversion of the individual C80-epoxide into the ω-terminal C77-aldehyde by treatment with H_5IO_6. The aldehyde was further subjected to reductive amination with 1-aminonaphthalene and $NaBH_4$ followed by phosphorylation with $Bu_4NH_2PO_4/CCl_3CN$ (Shibaev *et al*., 2000; Veselovsky *et al*., 2001a). In an analogous way, the derivative **2** was prepared from polyprenols of mulberry leaves (Veselovsky *et al*., 2001b), and polyprenols from birch trees were used for the synthesis of **1** (Veselovsky *et al*., 2001b).

The derivatives **4** and **5** which contain 1-aminonaphthalene residue at the γ-isoprene unit of the chain (Figure 2B) were synthesized as described (Grigorieva *et al*., 2000a), through directed aldol condensation to build the corresponding α,β-disubstituted acroleins, followed by their reductive amination and phosphorylation of the resulting amino alcohols.

The phosphates **1**–**5** were isolated as ammonium salts after ion exchange chromatography on DEAE-cellulose (DE-52, Whatman, acetate form) with elution by ammonium acetate in methanol. After concentration of the eluate, ammonium acetate was removed by precipitation with toluene. The products were characterized by NMR spectra (^{1}H, ^{13}C, and ^{31}P) and by mass spectra with electrospray ionization; for details, see the articles of Grigorieva *et al*. (2000b) and Veselovsky *et al*. (2001b).

All compounds were stored under nitrogen and at –20°C in the following organic solvents: **1** in heptane/2-propanol 4:1 (v/v) mixture, **2** in methanol, **3** in heptane/2-propanol 1.8:1.0 (v/v) mixture, **4** in heptane/2-propanol 1.15:1.00 (v/v) mixture, and **5** in hexane/2-propanol 3:1 (v/v) mixture. The choice of solvents for storage of these fluorescent Dol-P analogs was purely empirical and was based on a proper ratio of hexane to 2-propanol in order to achieve a good solubility of compounds. The concentration of the phosphates in these solutions was measured through determination of inorganic phosphate (Hess and Derr, 1975) after heating a sample with 57% $HClO_4$ for 15 min at 200°C. For the fluorescence studies, the organic solvent was evaporated under a nitrogen flow and replaced with 10 mM Tris–HCl buffer (pH 7.5), 0.15 M NaCl, 1 mM DTT, and 0.25% NP-40 (v/v). The solutions prepared were either used immediately or stored for up to several days at –80°C also under nitrogen.

Fluorescence measurements

Fluorescence intensity decays were determined in the time domain as described in our previous work (Xing *et al.*, 2000). Briefly, they were measured at 20 ± 0.1°C in an IBH 5000 photon-counting lifetime system equipped with a stable flash lamp operated at 40 kHz in 0.5 atm of hydrogen. For determination of intersite FRET distances between Trp133 and different fluorescent derivatives of bound substrate, the donor (Trp133) was excited at 295 nm and the quenching of the donor fluorescence in the presence of the acceptor (bound substrate derivatives, compounds **1**–**5**) was isolated at 340 nm. For the determination of the distance between Cys93 and the ω-end of the bound at the active site compound **1**, 1-aminonaphthalene fluorophore served as a fluorescence donor. It was excited at 340 nm, and quenching of the donor (1-aminonaphthalene) emission in the presence of the acceptor DAMBI covalently linked to Cys93 was isolated at 410 nm. The intensity decay data for each donor–acceptor pair were obtained from two DPM1Δ3 samples, one containing the donor only and the other containing both donor and acceptor, in a buffer containing 0.15 M NaCl, 10 mM Tris–HCl at pH 7.5, 1 mM DTT, and 0.01% NP-40. The two sets of lifetime data were used to calculate the distribution of the distances between donor and acceptor sites, using the program CFS_LS/GAUDIS (Dong *et al.*, 1997). The calculated results are displayed as a plot of the probability distribution of the distances, $p(r)$, assuming that the distribution is a Gaussian function. Non-stoichiometric labeling of acceptor site Cys93 by DAMBI was corrected in the calculation. In all studies of interactions with fluorescent substrates, detergent concentrations were kept at a minimum of <0.2% in order to minimize interference from adsorption of the detergent at wavelengths overlapping the excitation spectra of tyrosine and fluorescent derivatives.

Steady-state fluorescence was measured on an ISS PC1 photon-counting spectrofluorometer at 20 ± 0.1°C. Emission spectra were corrected for variation of the detector system with wavelength before they were used for determination of donor quantum yield and calculation of the spectral overlap integral. The Förster critical distance (R_o) at which the energy transfer efficiency is 0.5 was determined for each donor–acceptor pair under identical experimental conditions as for lifetime measurements. Fluorescent labeling of Cys93 with DAMBI was carried out as previously described (Xing *et al.*, 2000) in the presence of detergent, and the degree of labeling was >90%. All reported distances were derived from measurements of donor excited-state lifetimes. Donor intensity decay was analyzed by a model that includes a distribution function for the donor–acceptor distance. The analysis allows for the calculation of the mean distance of the distribution (McWherter *et al.*, 1986; Lakowicz *et al.*, 1988; She *et al.*, 1998; Lakowicz, 1999).

3D modeling

Yeast DPM1 protein alignments were constructed using Clustal W 1.82 (Thompson *et al.*, 1994). Secondary structure elements were predicted using PSI-PRED (Jones, 1999). Fold recognition analyses were carried out using the META server with the implemented 3Djury list (http://bioinfo.pl/Meta) (Ginalski *et al.*, 2003). Comparative/homology modeling of the enzyme was carried out at the Robetta Structure Prediction Server (http://robetta.bakerlab.org) (Chivian *et al.*, 2003b; Kim *et al.*, 2004). The Robetta algorithm found the X-ray crystal 3D structure of GT SpsA (pdb [3D structure depository] code: 1h7l) (Tarbouriech *et al.*, 2001) as the closest in structure to DPM1, and this structure was used as basis for homology modeling. The server returned five models, the first four representing the most populated clusters and the fifth the lowest energy structure outside those clusters. The models were assessed using the protein structure validation tools PROSA II (Sippl, 1993), VERIFY_3D (Eisenberg *et al.*, 1997), and ProQ (Wallner and Elofsson, 2003). The 3D structures and their properties were visualized with O (Jones *et al.*, 1991). The cartoon figures were obtained using PyMol (DeLano, 2003) and Grasp (Nicholls *et al.*, 1991) programs.

The model of the DPM1 complex with bound GDP-Man was obtained based on positioning this substrate as in the structurally homologous GT SpsA enzyme complex structure with dTDP in its active site cleft (pdb code: 1h7l) (Charnock and Davies, 1999; Tarbouriech *et al.*, 2001). Another substrate, Dol-P, was placed in the active site cleft based on complementarity of its geometry and complementarity of electrostatic and hydrophobic interactions. The 3D experimental (NMR-based) Dol-P coordinates were generously provided by Dr Frederick A. Troy II as published (Zhou and Troy 2003, 2005). All structures were aligned in 3D using the DALI server (http://www.ebi.ac.uk/dali) (Holm and Sander, 1998) and refined with refmac5 (Collaborative Computational Project, Number 4, 1994). The molecular manipulations were performed with moleman package as implemented in O graphics program (Jones *et al.*, 1991).

Acknowledgments

The authors thank Dr Frederic A. Troy II for providing the coordinates of C55-P Dol-P-like compound. This work was supported in part by United States Civilian Research and Development Foundation grant RN1-404 (V.N.S. and M.J.J.).

Conflict of interest statement

None declared.

Abbreviations

DAMBI, 4-dimethylaminophenylazophenyl-4′-maleimide; Dol-P, dolichyl-phosphate; Dol-P-Man, Dol-P mannose; dTDP, deoxythymidine 5′-diphosphate; DTT, dithiothreitol; ER, endoplasmic reticulum; GDP, guanosine 5′-diphosphate; GT, glycosyltransferase; GT-2, type 2 glycosyltransferase; IAEDANS, (5-iodoacetamidoethyl)aminonaphthalene-1-sulfonic acid; FRET, fluorescence resonance energy transfer; NP-40, Nonidet P40 (ethylphenylpolyethyleneglycol); SpsA, spore coat polysaccharide biosynthesis protein A; Tris, tris (hydroxymethyl)aminomethane; UDP, uridine 5′-diphosphate.

References

Babczinski, P. and Tanner, W. (1973) Involvement of dolicholmonophosphate in the formation of specific mannosyl-linkages in yeast glycoproteins. *Biochem. Biophys. Res. Commun.*, **54**, 1119–1124.

Banerjee, D.K., Carrasquillo, E.A., Hughey, P., Schutzbach, J.S., Martinez, J.A., and Baksi, K. (2005) *In vitro* phosphorylation by cAMP-dependent protein kinase up-regulates recombinant *Saccharomyces cerevisiae* mannosylphosphodolichol synthase. *J. Biol. Chem.*, **280**, 4174–4181.

Beck, P.J., Orlean, P., Albright, C., Robbins, P.W., Gething, M.J., and Sambrook, J.F. (1990) The *Saccharomyces cerevisiae* DPM1 gene encoding dolichol-phosphate-mannose synthase is able to complement a glycosylation-defective mammalian cell line. *Mol. Cell. Biol.*, **10**, 4612–4622.

Bujnicki, J.M., Elofsson, A., Fischer, D., and Rychlewski, L. (2001) Structure prediction meta server. *Bioinformatics*, **17**, 750–751.

Charnock, S.J. and Davies, G.J. (1999) Structure of the nucleotide-diphosphosugar transferase, SpsA from *Bacillus subtilis*, in native and nucleotide-complexed forms. *Biochemistry*, **38**, 6380–6385.

Chivian, D., Kim, D.E., Malmstrom, L., Bradley, P., Robertson, T., Murphy, P., Strauss, C.E., Bonneau, R., Rohl, C.A., and Baker, D. (2003a) Automated prediction of CASP-5 structures using the Robetta server. *Proteins*, **53** (Suppl. 6), 524–533.

Chivian, D., Kim, D.E., Malmstrom, L., Bradley, P., Robertson, T., Murphy, P., Strauss, C.E., Bonneau, R., Rohl, C.A., and Baker, D. (2003b) Automated prediction of CASP-5 structures using the Robetta server. *Proteins: Struct. Funct. Genet.*, **53** (Suppl. 6), 524–533.

Chojnacki, T., Palamarczyk, G., Jankowski, W., Krajewska-Rychlik, I., Szkopinska, A., and Vogtman, T. (1984) The enzymatic formation of dolichyl phosphate mannose from C-3 enantiomeric dolichyl phosphates. *Biochim. Biophys. Acta*, **793**, 187–192.

Collaborative Computational Project, Number 4 (1994) The CCP4 suite: programs for protein crystallography. *Acta Crystallogr., Sect. D: Cryst. Struct. Commun.*, **50**, 760–763.

Colussi, P.A., Taron, C.H., Mack, J.C., and Orlean, P. (1997) Human and *Saccharomyces cerevisiae* dolichol phosphate mannose synthases represent two classes of the enzyme, but both function in *Schizosaccharomyces pombe*. *Proc. Natl. Acad. Sci. USA*, **94**, 7873–7878.

DeLano, W.L. (2003) The PyMOL Molecular Graphics System. Available at: http://www.pymol.org. Accessed March 2005.

Dong, W.J., Chandra, M., Xing, J., She, M., Solaro, R.J., and Cheung, H.C. (1997) Phosphorylation-induced distance change in a cardiac muscle troponin I mutant. *Biochemistry*, **36**, 6754–6761.

Doucey, M.A., Hess, D., Cacan, R., and Hofsteenge, J. (1998) Protein C-mannosylation is enzyme-catalysed and uses dolichyl-phosphate-mannose as a precursor. *Mol. Biol. Cell*, **9**, 291–300.

Drickamer, K. and Taylor, M.E. (1998) Evolving views of protein glycosylation. *Trends Biochem. Sci.*, **23**, 321–324.

Eisenberg, D., Luthy, R., and Bowie, J.U. (1997) VERIFY3D: assessment of protein models with three-dimensional profiles. *Methods Enzymol.*, **277**, 396–404.

Ferguson, M.A. (1999) The structure, biosynthesis and functions of glycosylphosphatidylinositol anchors, and the contributions of trypanosome research. *J. Cell Sci.*, **112**, 2799–2809.

Forsee, W.T., McPherson, D., and Schutzbach, J.S. (1997) Characterization of recombinant yeast dolichyl mannosyl phosphate synthase and site-directed mutagenesis of its cysteine residues. *Eur. J. Biochem.*, **244**, 953–958.

Ginalski, K., Elofsson, A., Fischer, D., and Rychlewski, L. (2003) 3D-Jury: a simple approach to improve protein structure predictions. *Bioinformatics* **19**, 1015–1018.

Grigorieva, N.Y., Pinsker, O.A., Maltsev, S.D., Danilov, L.L., Shibaev, V.N., and Jedrzejas, M.J. (2000a) Dolichyl phosphate derivatives with a fluorescent label at an internal isoprene unit. *Mendeleev Commun.*, **3**, 221–251.

Grigorieva, N.Y., Pinsker, O.A., Maltsev, S.D., Danilov, L.L., Shibaev, V.N., and Jedrzejas, M.J. (2000b) Synthesis of dolichyl phosphates with fluorescent label in the γ-isoprene unit of the chain. *Russ. Chem. Bull. Intern. Ed.*, **49**, 2065–2071.

Hess, H.H. and Derr, J.E. (1975) Assay of inorganic and organic phosphorus in the 0.1–5 nanomole range. *Anal. Biochem.*, **63**, 607–613.

Holm, L. and Sander, C. (1998) Touring protein fold space with Dali/FSSP. *Nucleic Acids Res.*, **26**, 316–319.

Ilgoutz, S.C., Mullin, K.A., Southwell, B.R., and McConville, M.J. (1999) Evidence that free GPI glycolipids are essential for growth of *Leishmania mexicana*. *EMBO J.*, **18**, 2746–2755.

Imbach, T., Schenk, B., Schollen, E., Burda, P., Stutz, A., Grunewald, S., Bailie, N.M., King, M.D., Jaeken, J., Matthijs, G., and others. (2000) Deficiency of dolichol-phosphate-mannose synthase-1 causes congenital disorder of glycosylation type Ie. *J. Clin. Invest.*, **105**, 233–239.

Jedrzejas, M.J. and Setlow, P. (2001) Comparison of the binuclear metalloenzymes diphosphoglycerate-independent phosphoglycerate mutase and alkaline phosphatase: their mechanism of catalysis via a phosphoserine intermediate. *Chem. Rev.*, **101**, 607–618.

Jensen, J.W. and Schutzbach, J.S. (1985) Activation of dolichyl-phosphomannose synthase by phospholipids. *Eur. J. Biochem.*, **153**, 41–48.

Jensen, J.W. and Schutzbach, J.S. (1986) Characterization of mannosyltransfer reactions catalyzed by dolichyl-mannosyl-phosphate-synthase. *Carbohydr. Res.*, **149**, 199–208.

Jones, D.T. (1999) Protein secondary structure prediction based on position-specific scoring matrices. *J. Mol. Biol.*, **292**, 195–202.

Jones, T.A., Zou, J.Y., Cowan, S.W., and Kjeldgaard, M. (1991) Improved methods for binding protein models in electron density maps and the location of errors in these models. *Acta Crystallogr., Sect. A: Found. Crystallogr.*, **47**, 110–119.

Kim, D.E., Chivian, D., and Baker, D. (2004) Protein structure prediction and analysis using the Robetta server. *Nucleic Acids Res.*, **32**, W526–W531.

Kim, S., Westphal, V., Srikrishna, G., Mehta, D.P., Peterson, S., Filiano, J., Karnes, P.S., Patterson, M.C., and Freeze, H.H. (2000) Dolichol phosphate mannose synthase (DPM1) mutations define congenital disorder of glycosylation Ie (CDG-Ie). *J. Clin. Invest.*, **105**, 191–198.

Kinoshita, T., Ohishi, K., and Takeda, J. (1997) GPI-anchor synthesis in mammalian cells: genes, their products, and a deficiency. *J. Biochem.* (*Tokyo*), **122**, 251–257.

Kruszewska, J.S., Saloheimo, M., Migdalski, A., Orlean, P., Penttila, M., and Palamarczyk, G. (2000) Dolichol phosphate mannose synthase from the filamentous fungus *Trichoderma reesei* belongs to the human and *Schizosaccharomyces pombe* class of the enzyme. *Glycobiology*, **10**, 983–991.

Lakowicz, J.R. (eds) (1999) *Principle of Fluorescence Spectroscopy*. Kluwer Academic/Plenum Publishers, London, UK.

Lakowicz, J.R., Gryczynski, I., Cheung, H.C., Wang, C.K., Johnson, M.L., and Joshi, N. (1988) Distance distributions in proteins recovered by using frequency-domain fluorometry. Applications to troponin I and its complex with troponin C. *Biochemistry*, **27**, 9149–9160.

Lehle, L., Haselbeck, A., and Tanner, W. (1983) Synthesis of retinylphosphate mannose in yeast and its possible involvement in lipid-linked oligosaccharide formation. *Biochim. Biophys. Acta*, **757**, 77–84.

Maeda, Y., Tanaka, S., Hino, J., Kangawa, K., and Kinoshita, T. (2000) Human dolichol-phosphate-mannose synthase consists of three subunits, DPM1, DPM2 and DPM3. *EMBO J.*, **19**, 2475–2482.

Maeda, Y., Tomita, S., Watanabe, R., Ohishi, K., and Kinoshita, T. (1998) DPM2 regulates biosynthesis of dolichol phosphate-mannose in mammalian cells: correct subcellular localization and stabilization of DPM1, and binding of dolichol phosphate. *EMBO J.*, **17**, 4920–4929.

Mazhari-Tabrizi, R., Eckert, V., Blank, M., Muller, R., Mumberg, D., Funk, M., and Schwarz, R.T. (1996) Cloning and functional expression of glycosyltransferases from parasitic protozoans by heterologous complementation in yeast: the dolichol phosphate mannose synthase from *Trypanosoma brucei brucei*. *Biochem. J.*, **316**, 853–858.

McWherter, C.A., Haas, E., Leed, A.R., and Scheraga, H.A. (1986) Conformational unfolding in the N-terminal region of ribonuclease A detected by nonradiative energy transfer. *Biochemistry*, **25**, 1951–1963.

Murgolo, N.J., Patel, A., Stivala, S.S., and Wong, T.K. (1989) The conformation of dolichol. *Biochemistry*, **28**, 253–260.

Nicholls, A., Sharp, K.A., and Honig, B. (1991) Protein folding and association: insights from the interfacial and thermodynamic properties of hydrocarbons. *Proteins: Struct. Funct. Genet.*, **11**, 281–296..

Nozaki, M., Ohishi, K., Yamada, N., Kinoshita, T., Nagy, A., and Takeda, J. (1999) Developmental abnormalities of glycosylphosphatidylinositol-anchor-deficient embryos revealed by Cre/loxP system. *Lab. Invest.*, **79**, 293–299.

Orlean, P. (1992) Enzymes that recognize dolichols participate in three glycosylation pathways and are required for protein secretion. *Biochem. Cell Biol.*, **70**, 438–447.

Orlean, P., Albright, C., and Robbins, P.W. (1988) Cloning and sequencing of the yeast gene for dolichol phosphate mannose synthase, an essential protein. *J. Biol. Chem.*, **263**, 17499–17507.

Pace, C.N., Vajdos, F., Fee, L., Grimsley, G., and Gray, T. (1995) How to measure and predict the molar absorption coefficient of a protein. *Protein Sci.*, **4**, 2411–2423.

Palamarczyk, G., Lehle, L., Mankowski, T., Chojnacki, T., and Tanner, W. (1980) Specificity of solubilized yeast glycosyl transferases for polyprenyl derivatives. *Eur. J. Biochem.*, **105**, 517–523.

Palamarczyk, G., Vogtman, T., Chojnacki, T., Bause, E., Mizuno, M., and Takigawa, K. (1987) Enantiomeric forms of phospho-2,3-dihydroprenols in mannosyl transfere. *Chem. Scr.*, **27**, 135–136.

Rush, J.S., Panneerselvam, K., Waechter, C.J., and Freeze, H.H. (2000) Mannose supplementation corrects GDP-mannose deficiency in cultured fibroblasts from some patients with Congenital Disorders of Glycosylation (CDG). *Glycobiology*, **10**, 829–835.

Saxena, I.M., Brown, R.M. Jr, Fevre, M., Geremia, R.A., and Henrissat, B. (1995) Multidomain architecture of beta-glycosyl transferases: implications for mechanism of action. *J. Bacteriol.*, **177**, 1419–1424.

Schenk, B., Fernandez, F., and Waechter, C.J. (2001) The ins(ide) and out (side) of dolichyl phosphate biosynthesis and recycling in the endoplasmic reticulum. *Glycobiology*, **11**, 61R–70R.

Schutzbach, J.S. (1994) Is there a 'dolichol recognition sequence' in enzymes that interact with dolichols and other polyisoprenoid substrates? *Acta Biochim. Pol.*, **41**, 269–274.

Schutzbach, J.S. (1997) The role of the lipid matrix in the biosynthesis of dolichyl-linked oligosaccharides. *Glycoconj. J.*, **14**, 175–182.

Schutzbach, J.S., Zimmerman, J.W., and Forsee, W.T. (1993) The purification and characterization of recombinant yeast dolichyl-phosphate-mannose synthase. Site-directed mutagenesis of the putative dolichol recognition sequence. *J. Biol. Chem.*, **268**, 24190–24196.

She, M., Xing, J., Dong, W.J., Umeda, P.K., and Cheung, H.C. (1998) Calcium binding to the regulatory domain of skeletal muscle troponin C induces a highly constrained open conformation. *J. Mol. Biol.*, **281**, 445–452.

Shibaev, V.N. and Danilov, L.L. (1997) Synthesis of intermediates in the dolichol pathway of protein glycosylation. In Large, D.G. and Warren, C.D. (eds), *Glycopeptides and Related Compounds: Synthesis, Analysis, and Applications*. Marcel Dekker Inc, New York, Basel, Hong Kong, pp. 427–504.

Shibaev, V.N., Veselovsky, V.V., Lozanova, A.V., Maltsev, S.D., Danilov, L.L., Forsee, W.T., Xing, J., Cheung, H.C., and Jedrzejas, M.J. (2000) Synthesis of dolichyl phosphate derivatives with fluorescent label at the omega-end of the chain, new tools to study protein glycosylation. *Bioorg Med. Chem. Lett.* **10**, 189–192.

Sippl, M.J. (1993) Recognition of errors in three-dimensional structures of proteins. *Proteins*, **17**, 355–362.

Tanner, W. (1969) A lipid intermediate in mannan biosynthesis in yeast. *Biochem. Biophys. Res. Commun*, **35**, 144–150.

Tarbouriech, N., Charnock, S.J., and Davies, G.J. (2001) Three-dimensional structures of the Mn and Mg dTDP complexes of the family GT-2 glycosyltransferase SpsA: a comparison with related NDP-sugar glycosyltransferases. *J. Mol Biol.*, **314**, 655–661.

Thompson, J.D., Higgins, D.G., and Gibson, T.J. (1994) CLUSTAL W: improving the sensitivity of progressive multiple sequence alignment through sequence weighting, position-specific gap penalties and weight matrix choice. *Nucleic Acids Res.*, **22**, 4673–4680.

Tomita, S., Inoue, N., Maeda, Y., Ohishi, K., Takeda, J., and Kinoshita, T. (1998) A homologue of *Saccharomyces cerevisiae* Dpm1p is not sufficient for synthesis of dolichol-phosphate-mannose in mammalian cells. *J. Biol. Chem.*, **273**, 9249–9254.

Veselovsky, V.V. (1999) A simple method for preparing racemic dolichols from the polyprenols of pine needles (*Pinus silvestris*). *Russ. Chem. Bull. Intern. Ed.*, **48**, 1000–1001.

Veselovsky, V.V. and Lozanova, A.V. (2000) A new version of the conversion of plant polyprenols into (+/-)-terpenols of dolichol series. *Russ. Chem. Bull. Intern. Ed.*, **49**, 1485–1486.

Veselovsky, V.V., Lozanova, A.V., Maltsev, S.D., Danilov, L.L., Shibaev, V.N., and Jedrzejas, M.J. (2001a) Dolichyl phosphate derivatives with fluorescent labels. Analogs of dolichyl phosphate with 2-aminopyridine residue at the ω-end of the chain. *Russ Chem. Bull. Intern. Ed.*, **50**, 531–536.

Veselovsky, V.V., Lozanova, A.V., Maltsev, S.D., Danilov, L.L., Shibaev, V.N., and Jedrzejas, M.J. (2001b) Dolichyl phosphate derivatives with fluorescent labels. Analogs of dolichyl phosphate with different isoprene chain length containing 1-aminonaphthalene residue at the ω-end of the chain. *Russ. Chem. Bull. Intern. Ed.*, **50**, 2121–2126.

Wallner, B. and Elofsson, A. (2003) Can correct protein models be identified? *Protein Sci.*, **12**, 1073–1086.

Wilson, I.B., Taylor, J.P., Webberley, M.C., Turner, N.J., and Flitsch, S.L. (1993) A novel mono-branched lipid phosphate acts as a substrate for dolichyl phosphate mannose synthetase. *Biochem. J.*, **295**, 195–201.

Xing, J., Forsee, W.T., Lamani, E., Maltsev, S.D., Danilov, L.L., Shibaev, V.N., Schutzbach, J.S., Cheung, H.C., and Jedrzejas, M.J. (2000) Investigations of the active site of *Saccharomyces cerevisiae* dolichyl-phosphate-mannose synthase using fluorescent labeled dolichyl-phosphate derivatives. *Biochemistry*, **39**, 7886–7894.

Zhou, H.X. and Shan, Y. (2001) Prediction of protein interaction sites from sequence profile and residue neighbor list. *Proteins: Struct. Funct. Genet.*, **44**, 336–343.

Zhou, G.P. and Troy, F.A., II. (2003) Characterization by NMR and molecular modeling of the binding of polyisoprenols and polyisoprenyl recognition sequence peptides: 3D structure of the complexes reveals sites of specific interactions. *Glycobiology*, **13**, 51–71.

Zhou, G.P. and Troy, F.A., II. (2005) NMR study of the preferred membrane orientation of polyisoprenols (dolichol) and the impact of their complex with polyisoprenyl recognition sequence peptides on membrane structure. *Glycobiology*, **15**, 347–359.

Zimmerman, J.W. and Robbins, P.W. (1993) The hydrophobic domain of dolichyl-phosphate-mannose synthase is not essential for enzyme activity or growth in Saccharomyces cerevisiae. *J. Biol. Chem.*, **268**, 16746–16753.

Zimmerman, J.W., Specht, C.A., Cazares, B.X., and Robbins, P.W. (1996) The isolation of a Dol-P-Man synthase from *Ustilago maydis* that functions in *Saccharomyces cerevisiae*. *Yeast*, **12**, 765–771.